PROJECTED TRENDS IN CLIMATE EXTREMES IN THE PASSAIC RIVER BASIN BASED ON CMIP5 BIAS-CORRECTED AND SPATIALLY DOWNSCALED GENERAL CIRCULATION MODEL SIMULATIONS

A. Prasad* and C. Alo
Department of Earth and Environmental Studies
Montclair State University
1 Normal Avenue
Montclair, NJ 07043

ABSTRACT: *General Circulation Models (GCMs) are useful tools for estimating future climatic changes. GCMs typically employ data at large spatial scales and can be useful in determining changes for large areas; however, these changes may differ regionally. By downscaling and bias correcting GCM outputs, more accurate projections concerning smaller regions can be made. The Multivariate Adaptive Constructed Analogs (MACA) models provide daily precipitation and temperature information for point localities by modifying coarse resolution data from GCMs to a higher spatial resolution. In this study, trends in climate extremes over the Passaic River Basin (PRB) between 1981-2005 are estimated based on three MACA-modified models (bcc-csm1-1m, CCSM4, and MRI-CGCM3). The historical trends obtained from the MACA models are validated using an observational dataset and statistically further corrected to adjust for bias. Projected trends for 2051-2075 relative to the 1981-2005 baseline dataset are investigated.*

Keywords: *climate modeling, climate change projections, bias correction, MACA, Passaic River Basin*

INTRODUCTION

Climatic patterns are expected to drastically change across the globe within the century. 1983-2012 proved to be the hottest 30-year period on record for the northern hemisphere in the last 1400 years, with this trend continuing to present day; 2020 was the warmest year on record, tying with 2016 (IPCC, 2013; NASA, 2021). Extreme heat is the leading weather-related cause of death, and is exacerbated in urban areas (Peterson et al., 2013). The Northeastern United States—home to nearly 50 million residents in the urban "Northeast Megalopolis" composed of the sprawling area from Boston to Washington, D.C.—has already experienced an overall increase in temperatures by nearly 2˚F, increased frequency of precipitation events, with a near 70% increase in amount of precipitation during heavy precipitation events, and is expected to see longer summers, warmer winters, more temperature extremes in the winter and summer, as well as increased occurrence of droughts despite expectations of more frequent, heavier wet-weather events (Florida, 2019; US EPA, 2017; Karl et al., 2009). An increase in frequency and intensity of precipitation events can lead to more flash floods in the summer, especially in urban areas ill-prepared for these events, while increased winter precipitation can increase flooding associated with warm temperatures combining precipitation runoff and snowmelt to overwhelm water systems (Khajehei et al., 2020; Ouellet et al., 2012). Assessing change in departures from general historical climate trends can have long reaching benefits towards mitigation of the potential damage of climate change.

Evaluating potential changes in future climate extremes can be a useful way of determining the wide-ranging impacts of climate change. Germain and Lutz (2020), for example, argue that these extreme indices could be more important in determining changing ranges of species than climate means. Vogel et al. (2019) find that extremes of droughts or heat waves can have significant implications for agricultural yields, threatening global food security and North American production of maize, wheat, and soy. Investigating these trends in depth has undeniable value. Studies may assess extreme climate indices as part of their analysis of changes in climate extremes, using Regional Climate Models to compare climate extremes from a baseline historic period against the projected future data (Marengo et al., 2009; Thibeault and Seth, 2004). The full range of climate extremes, based on temperature and precipitation data, has been defined by the Expert Team on Climate Change Detection and Indices (ETCCDI) and is available in Zhang et al. (2011) and at http://etccdi.pacificclimate.org/list_27_indices.shtml. From the 27 available indices, we follow Marengo et al. (2009) in calculating six indices that do not include very rare events, but nonetheless provide insight towards extreme events. These indices include the percentage of time in which the daily minimum temperature is

below the 10th percentile (TN10p), percentage of time in which the daily minimum temperature is greater than the 90th percentile (TN90p), maximum number of consecutive days when precipitation is less than 1 mm (CDD), annual count of days when precipitation is greater than 10 mm (R10), monthly maximum consecutive 5-day precipitation (Rx5day), and annual total precipitation from days in which precipitation amounts are above than the 95th percentile (R95p) (see Table 1).Although the effects of climate change on large areas can be estimated using General Circulation Models (GCMs), GCMs contain significant biases—including an established underestimation of dry days and difficulty projecting extreme precipitation events—and are too coarse for basin-level studies (Sharma et al., 2007; Dai, 2006; Leander and Buishand, 2007). Furthermore, because of the variation of climate models, it is generally recommended to use multiple models when using the forecasting data (Murphy et al., 2004; IPCC, 2007). Therefore, to project climate change impacts at a finer resolution, using data from multiple Regional Climate Models (RCMs) may be beneficial. In order to make large-scale, coarse datasets more representative to local climate, RCMs downscale historical and future projections under different emissions scenarios.

Table 1. Climate indices used in this study, taken from Zhang et al. (2011).

ID	Indicator Name	Indicator Definition	Unit
TN10p	Cool nights	Percentage of time when daily min temperature < 10th percentile	%
TN90p	Warm nights	Percentage of time when daily min temperature > 90th percentile	%
CDD	Consecutive dry days	Maximum number of consecutive days when precipitation < 1 mm	Days
R10	Number of heavy precipitation days	Annual count when precipitation ≥ 10 mm	Days
Rx5day	Max 5-day precipitation amount	Monthly maximum consecutive 5-day precipitation	mm
R95p	Very wet days	Annual total precipitation from days > 95th percentile	mm

The Passaic River Basin (PRB) encompasses and drains approximately 935 square miles of land largely in New Jersey and partially in southern New York State (Figure 1). Nestled in the basin is the Passaic River, which empties out into the Newark Bay at 80 miles (129 kilometers) from the source. The PRB is one of the most densely populated regions in New Jersey and provides nearly 66% of New Jersey residents with clean drinking water. The PRB is particularly vulnerable to climate extremes such as floods and heat waves and therefore, expected changes in climate extremes are therefore of particular concern for the PRB.

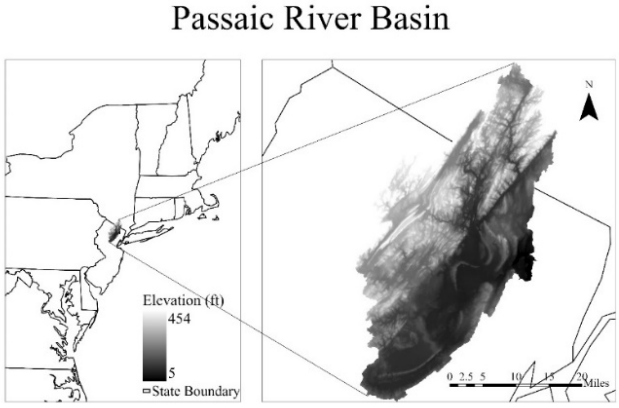

Figure 1. Elevation map of the Passaic River Basin, located in New Jersey and New York State.

This paper investigates the usefulness of applying MACA data to investigate the impacts of climate change in the whole of the PRB under the medium-emission Representative Concentration Pathway (RCP) 4.5 and the high-emissions scenario RCP 8.5 after performing further bias correction. The study looks at ways in which the PRB will experience precipitation and temperature changes according to climate model projections. We explore changes in (1) TN10p, (2) TN90p, (3) CDD, (4) R10, (5), Rx5day, and (6) R95p in 2051-2075 against our baseline 1981-2005 data. Identifying future changes in the PRB with respect to the coldest nights, warmest nights, consecutive dry days, rainy days in which precipitation exceeds 10 mm, the 95th percentile of precipitation, and the yearly maximum consecutive 5-day precipitation can be useful to planners and policy makers to help communities increase their resilience against climate change.

DATA AND METHODS

Climate data is provided by the MACA model, developed at the University of Idaho (Abatzouglou, 2013). For purposes of this study, three climate models were chosen to provide historical and future model climate data: (1) bcc-csm1-1m, (2) MRI-CGCM3, and (3) CCSM4. These models represent 3 of 30 ranked GCMs, all of which have significantly differing normalized error score. Observational data required for bias-correction was available from the USGS but limited for our study area. Precipitation and temperature data taken from the Parameter-elevation Regressions on Independent Slopes Model (PRISM) was highly correlated with available USGS data (r = 0.83-0.99), and therefore, the PRISM model was chosen as an acceptable alternative to observational data.

Data obtained from downscaling, the process of extrapolating large-resolution data to a finer scale, must be approached with some amount of uncertainty due to limitations from the GCMs and consequently bias corrected if they are to be at all realistic; issues linked with using model data that has not been bias-corrected include underestimation of dry days, overestimation of wet days, and inability to include high precipitation events (Piani et al., 2010). Bias correction is required when working with climate models, especially for the temperature and precipitation variables (Christensen et al., 2008; Li et al., 2010; Watanabe et al., 2012). Several statistical methods exist to bias correct these timeseries data, but these must be employed with caution as well in order to avoid an underestimation of climate extremes in the future emissions scenarios (Li et al., 2010).

Of the statistical bias correction methods available and validated in the literature, we explore the methods of quantile mapping and the delta change method. Quantile mapping and the delta change methods are respectively two of the more common approaches of correcting climate model data. Quantile mapping is cited as outperforming other bias correction approaches (Lafon et al., 2013; Räty et al., 2014). With this method, trends in simulated precipitation and temperature are noted to be better preserved (Ngai et al., 2017). However, this method can outperform others based on variables such as seasonality and location (Räty et al., 2014). Therefore, we also examine the usefulness of the delta change method of correcting bias, which scales historic climate data against observed values and applies a change factor to future data. The delta-change method is a reliable method of correction since it uses observed data as a baseline to correct mean model values (Mendez et al., 2020). We look to assess the usefulness of these climate data in the Passaic River Basin.

Quantile mapping for bias-correction of model data is transformed by an inverse cumulative distribution function (CDF):

$$\hat{x}_m(t) = F_O^{-1}[F_m\{x_M(t)\}] \quad (1)$$

where $\hat{x}_m(t)$ is the bias-corrected data, $x_m(t)$ is the model data, F_O^{-1} is the inverse of the observed CDF and F_m is the model CDF (Eum, et al., 2017). This formula helps shift the modeled values to more closely match the observed values based on the cumulative probability of occurrence. This method suggests that when the model CDFs more closely match the observed, the values and resulting analysis have greater credibility. Comparing the CDFs of observed and model data can be helpful in proving the reliability of employed correction methods.

To perform the bias correction for precipitation through the delta change method, corrections are made by a multiplicative factor consisting of the ratio between observed and model values applied to daily observed values:

$$c = \frac{\sum_{i=1}^{n} P_i^{obs}}{\sum_{i=1}^{n} P_i^{model}} \quad (2)$$

$$\widetilde{P_{ij}}^{model} = c * P_{ij}^{model} \quad (3)$$

where c is the correction factor, P_i^{obs} is the mean monthly observed precipitation, P_i^{model} is the monthly mean of the model value of precipitation, and $\widetilde{P_{ij}}^{model}$ is a daily timeseries value for the corrected model data (Hempel et al., 2013). This method, although simple, is useful in correcting precipitation data. In using the correction factor, a monthly mean over the baseline period is calculated and applied to daily values (Chen et al., 2013).

Temperature is corrected through additive correction:

$$C = \frac{1}{n}(\sum_{i=1}^{n} T_i^{obs} - \sum_{i=1}^{n} T_i^{model}) \quad (4)$$

$$\widetilde{T_{ij}}^{model} = C + T_{ij}^{model} \quad (5)$$

where C is the correction factor, n is the total number of days in the defined time period, T_i^{obs} is the observed temperature at day *i*, T_i^{model} is the modeled output temperature at day *i*, and $\widetilde{T_{ij}}^{model}$ is the corrected temperature at day *i* in month *j* (Hempel, et al., 2013).

RESULTS AND DISCUSSION

Data Analysis

Historical data

Because of limited available historical data, we use the PRISM dataset, available at https://prism.oregonstate.edu/explorer/. Validation of data was performed by checked daily correlation of model data against the limited observed data. Comparing daily PRISM values to the USGS data shows R^2 ranging from 0.83-0.99 in selected locations in the PRB. Therefore, PRISM is chosen to provide observational values.

Precipitation bias correction

Though the MACA datasets include bias-correction, further correction was performed due to low correlations between MACA data and the observed data set (r = 0.63-0.73). After further correction, these values improved to 0.97-0.99 (Figure 2). Assessment of precipitation data through CDF comparison is utilized to determine which of the bias-correction methods is the most reliable for this data set. Comparing the CDF of each bias-corrected data against the raw data CDF is used to validate data (Figure 3). A clear distinction exists between the CDFs for PRISM and bcc-csm1-1m, which overestimates precipitation.

Figure 3 shows the CDFs of PRISM, delta change correction factor (CF) MACA data, raw MACA data, and the quantile mapping corrected MACA data. The cumulative distribution of the precipitation data for all three models is overestimated through the quantile mapping transformation. However, the improvement of the delta method corrected MACA model against the raw model CDF is noteworthy. Though the differences are slight between the respective models, the distribution of the delta change method CDFs most closely match that of the PRISM model.

In comparing the raw average precipitation for June, July, and August (JJA) and December, January, and February (DJF) against the corrected values for the respective months, there is a clear distinction between the two graphs (see Figure 2). Raw model precipitation in particular shows disagreements between the models by month for the winter months, whereas the summer months show more cohesive, united results. The models in general overestimate precipitation in comparison to the PRISM values. After correction, the monthly averages match PRISM much more significantly; the correlation coefficients of bias corrected, summer precipitation data increases to 0.97-0.98 from 0.63-0.73. The accuracy at the monthly scale validates that MACA can be utilized in reasonably projecting seasonal-scale climate shifts with further bias correction.

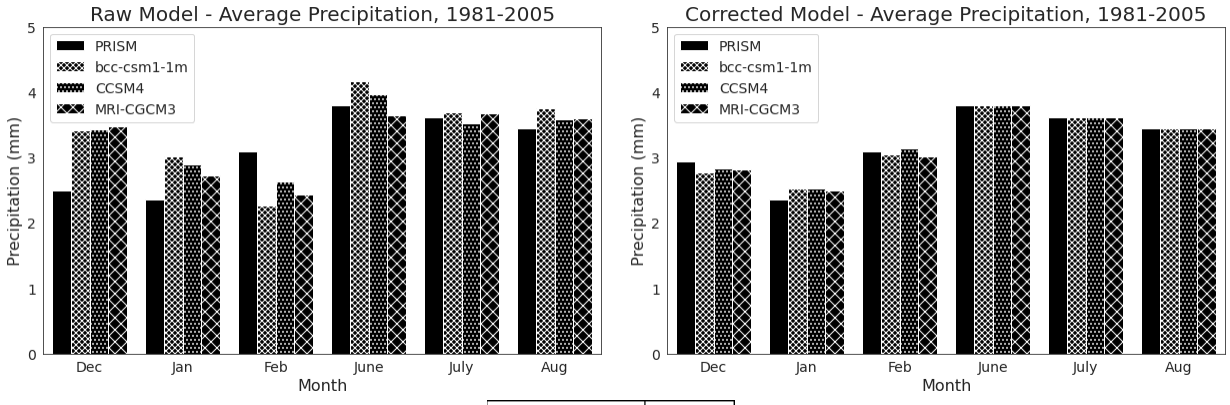

Correlation	r
Prism/raw bcc	0.63259371
Prism/raw CCSM4	0.73634863
Prism/raw MRI	0.68893687
Prism/CF bcc	0.97973767
Prism/CF CCSM4	0.98885205
Prism/CF mri	0.98510118

Figure 2. Comparison of seasonal average precipitation for winter and summer months with correlations for a sample location in the PRB.

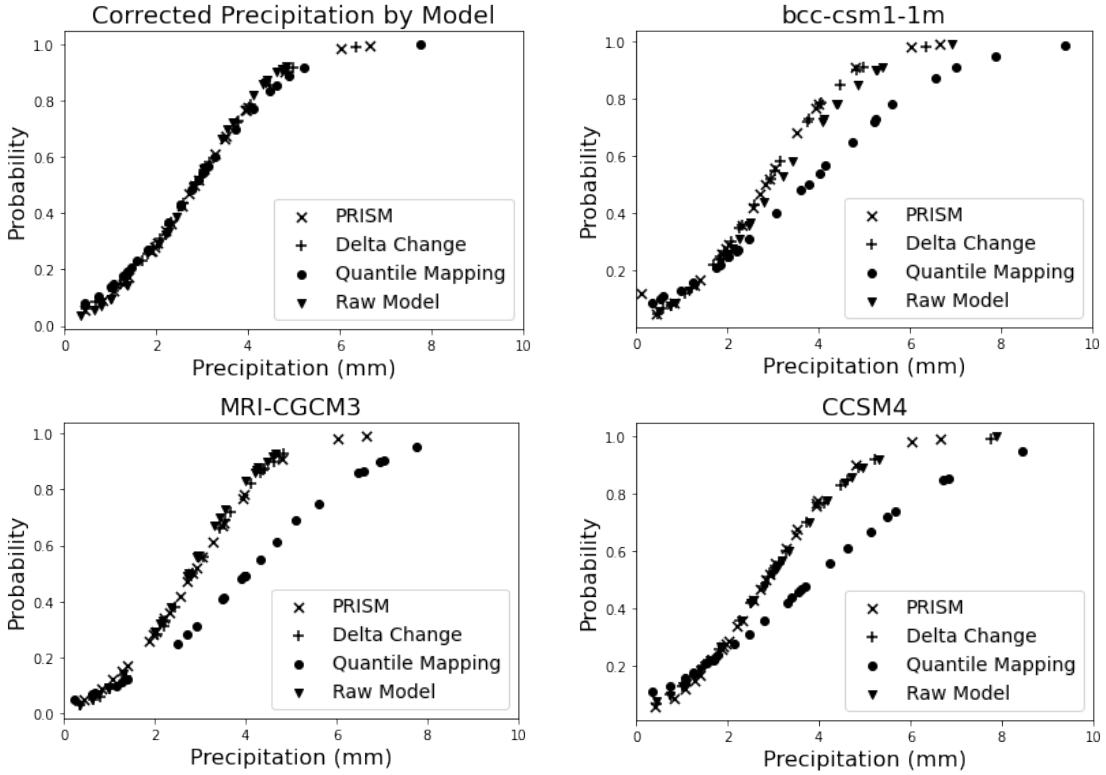

Figure 3. CDFs of the raw data and corrected data against PRISM for a sample location in the PRB.

Temperature

Bias-correction improves precipitation values, but temperature bias-correction executed through the linear additive method decreases the correlation coefficient in several cases. Because the correlations are either made worse or not significantly improved, the additive method is not considered a reliable method of temperature bias-correction

for this study. The correlation between PRISM and the models for the summer and winter months is 0.99 for both, Tmin and Tmax (see Figure 4). Despite the slightly lower correlation with daily temperature, raw MACA temperature values are considered satisfactory for the purposes of this study.

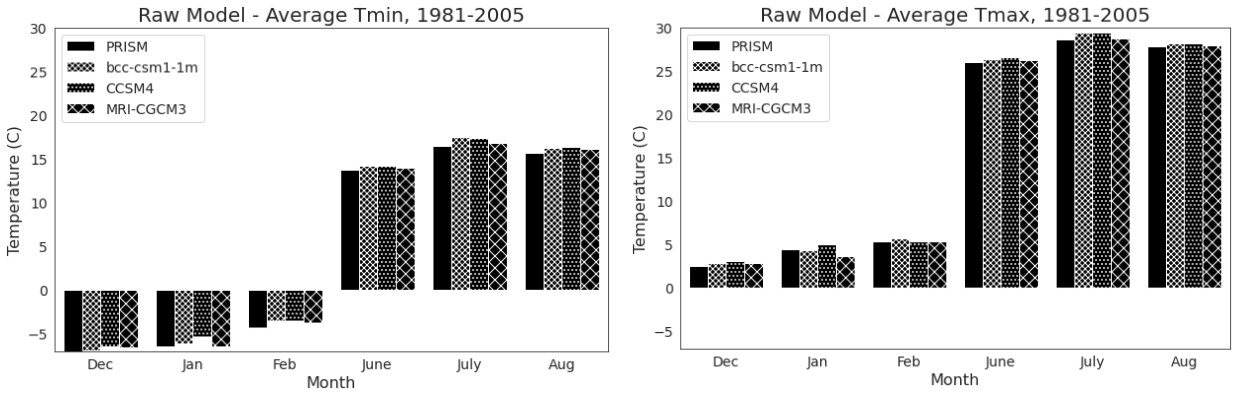

Tmin Correlation	r
Prism/raw bcc	0.99980091
Prism/raw CCSM4	0.999906
Prism/raw MRI	0.99955994

Tmax Correlation	r
Prism/raw bcc	0.99981235
Prism/raw CCSM4	0.99985332
Prism/raw MRI	0.99951523

Figure 4. Monthly minimum and maximum temperature comparison.

Climatology

Very cold nights, TN10p, represent the bottom 10th percentile of nightly temperatures. By looking at the historic trends in TN10p, a general established pattern can be compared to future trends Though the models disagree about exactly when the percentage of cold nights decrease—PRISM, bcc-csm1-1m, and CCSM4 all mark this general downward trend turning point around 1994—they all show a decrease in total percentage of very cold nights. For the future projections, the models vary in output for the predicted cold nights. The models all agree that the amount of very cold nights will decrease, but at different rates dependent on the scenario used. These differences are shown very distinctly in Table 2. CCSM4 and bcc-csm1-1m both agree that in scenario 4.5, there will be a decrease of about 0.1%, whereas scenario 4.5 for MRI-CGCM3 predicts a difference of approximately -0.25%. Interestingly, both bcc-csm1-1m and MRI-CGCM3 both project that in RCP 8.5—the scenario in which emissions are widely unregulated—the TN10p will decrease to almost half of the respective predictions in RCP 4.5.

Table 2. Future changes in extreme climate indices to the PRB (2051-2075 minus 1981-2005).

	Δ TN10p (%)	**Δ TN90p (%)**	**Δ CDD (days)**	**Δ R10 (days)**	**Δ R95p (mm)**	**Δ Rx5day (mm)**
Bcc-csm1-1m RCP 4.5	- 0.11%	0.05%	0.20	- 0.30	33	18
Bcc-csm1-1m RCP 8.5	- 0.06%	0.05%	0.70	1.70	72	30.5
CCSM4 RCP 4.5	- 0.12%	0.03%	- 0.51	1.48	25	5.5
CCSM4 RCP 8.5	- 0.24%	- 0.07%	- 0.48	1.70	63	30.5
MRI-CGCM3 RCP 4.5	- 0.25%	0.11%	- 2.19	0.47	- 1	-1
MRI-CGCM3 RCP 8.5	- 0.13%	0.17%	- 1.89	3.40	68	47

Very warm nights, TN90p, represent the 90th percentile of minimum temperatures. In assessing changes in TN90p from 2051-2075 as compared to our baseline 1981-2005, there is an overall increase in the anomalies for the warmest nights. Though there are a few dips in the moving average through the years, which may be partially attributed to the El Niño/La Niña phenomenon (Yun et al., 2016), the overall trend shows an increase in percentage of days in which the minimum temperature is greater than 90% of total temperatures. For future projections, the model output for change in TN90p is overall somewhat more in line with expectations for change in the PRB. Theoretically, RCP 8.5 should have a larger increase in the number of warm nights; however, bcc-csm1-1m interestingly predicts that in both scenarios, there will be an approximate 0.25% increase in warm nights. CCSM4 presents an outlier and predicts that scenario 8.5 will have an overall decrease in warm nights. MRI-CGCM3 represents the expected outcome with RCP 8.5 showing a drastic increase in the warm nights over RCP 4.5. Despite the variations, 5 out of 6 future scenarios agree that there will be an increase in warm nights.

Consecutive dry days (CDD) are the maximum count of days in which the precipitation is less than 1 mm. bcc-csm1-1m predicts a low number of consecutive dry days because of the overestimation of precipitation, which is clear in the cumulative distribution comparison against PRISM data. Unsurprisingly, the distribution of consecutive dry days shows that the models predict varying outcomes for total change in CDD. Bcc-csm1-1m is the only model that conforms to available literature that estimates that New Jersey and the mid-Atlantic states are projected to see more frequent droughts despite heavier and more frequent precipitation. The other models show a decrease in CDD in comparison to their historical counterparts. While looking at the actual expected change between the average CDD relative to the historical CDD, MRI-CGCM3 and corrected CCSM4 show unexpected results. MRI-CGCM3 shows an overall decrease in CDD in RCPs 4.5 and 8.5, whereas bcc-csm1-1m 8.5 shows an increase in overall consecutive dry days. Raw data from CCSM4 shows no change between RCP 8.5 and the historical value for CDD, while the corrected version of the data shows a decrease in CDD.

The differences in the distribution of days in which precipitation amounts to over 10 mm (R10) data between the 3 modeled projections do not drastically differ. CCSM4 shows that the 50th percentile of R10 days differs by approximately 2 days, but the maximum number of days is approximately the same between the historic and future scenarios. Bcc-csm1-1m shows the most difference in distribution of data, with the full range of historic raw data extending from 30-55 days, RCP 4.5 ranging from 21-50 days, and RCP 8.5 ranging from 23-60 days. CCSM4 shows all climate scenarios with the same maximum value, while minimum values range from 22-26 days. The difference in data from MRI-CGCM3 between the historic and future emissions scenarios is insignificant.

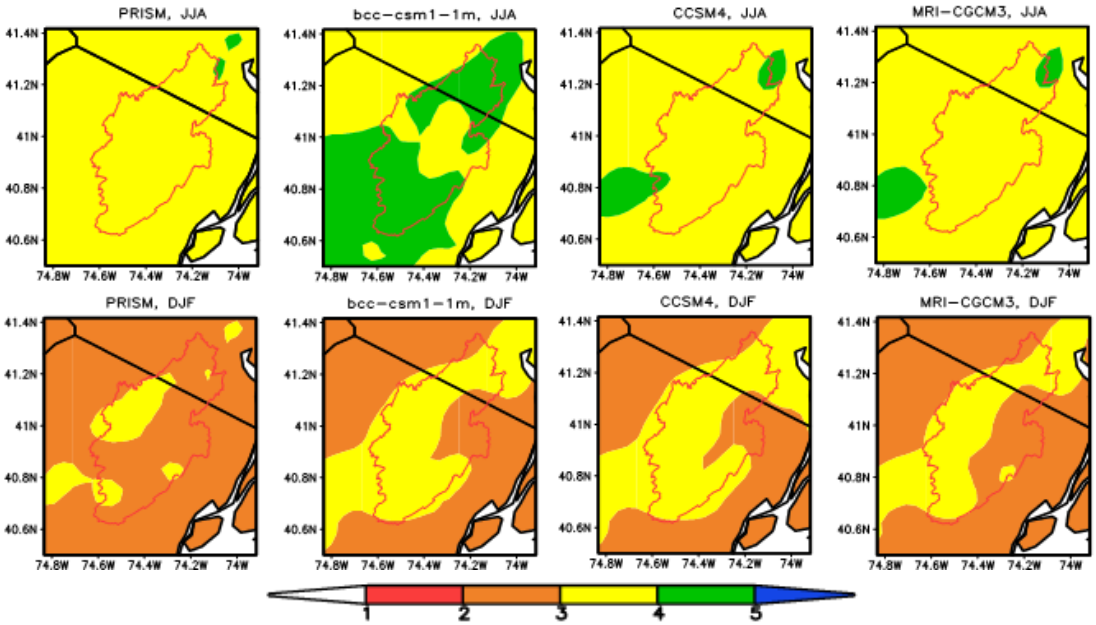

Figure 5. Average historical (1981-2005) summer and winter precipitation (mm/day) from observed (PRISM) and MACA models.

Examining the total change between the future average compared to the historical R10, the models agree that there is an expected increase in total days in which the precipitation falls over 10 mm in RCP 8.5. However, RCP 4.5 has mixed output. Bcc-csm1-1m shows a decrease in precipitation in comparison to the baseline time period for RCP 4.5, CCSM4 shows an increase of only 1-1.5 days, and MRI-CGCM3 shows a decrease for the raw data and an increase for the corrected data. The plots in Figure 5 show average precipitation amounts for the winter and summer months. Though there are differences between the models, with the overestimation of bcc-csm1-1m summer precipitation clear, most of the PRB (outlined in red) shows summer precipitation to fall between 3-5 mm.

Winter months show average precipitation to historically be between 2 and 4 mm. However, when looking at the average expected R10 from RCP 8.5, the models heavily disagree (see Figure 6). Bcc-csm1-1m shows the full range of values available, while MRI-CGCM3 is only slightly more varied, with a range from 10-70 days per year. CCSM4, on the other hand, shows the whole PRB to experience more than 70 days in which precipitation is greater than 10 mm.

For R95p, the extremes in PRISM most closely match those of CCSM4. MRI-CGCM3 and bcc-csm1-1m both have extreme precipitation predictions on lower scales, whereas CCSM4 and PRISM have high precipitation values close to 300 mm above the average and low values near 200 below the average. The expected change between the historic average R95p and the historic R95p is relatively united amongst the models. In RCP 8.5, each of the models anticipate a minimum of 30 mm of intense precipitation, with a maximum of nearly 80 mm. RCP 4.5 sees a slightly more varied distribution of data, but all models except MRI-CGCM3 see an increase in average R95p. In most of these climate scenarios, the amount of intense precipitation will increase significantly.

The yearly maximum consecutive 5-day precipitation, Rx5day, is the final climate index marker analyzed in this study. The monthly maximum 5-day precipitation addresses the frequency of precipitation whereas the other climate indices related to precipitation address the absence of precipitation or the amount. The models agree in RCP 8.5 that the maximum 5-day precipitation amount will increase, with values of precipitation ranging from 20 mm to approximately 48 mm. As with the R95p, bcc-csm1-1m and CCSM4 also agree—albeit bcc-csm1-1m predicts nearly 4 times the intensity of CCSM4—that the Rx5day will increase in scenario 4.5, while MRI-CGCM3 predicts decreases in the frequency of consecutive rainy days.

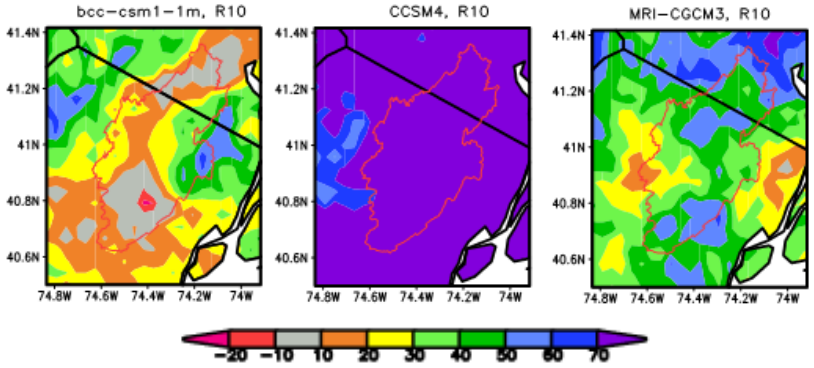

Figure 62 - Projected changes in heavy wet-weather days in which precipitation is greater than 10 mm (R10) in RCP 8.5.

Plotting seasonal changes over the PRB provides more in-depth analysis. Figure 7 shows average Rx5day amounts, providing further insight to the expected changes in the PRB for scenario RCP 8.5. Bcc-csm1-1m presents a gradient of change with average precipitation decreasing in increments of 10 mm towards the east. All the models seem to agree that the areas further east will experience lower extreme rainfall than the western regions. Bcc-csm1-1m and MRI-CGCM3 both expect the easternmost regions along the border of the PRB will experience less amounts of total average precipitation in the 2051-2075. These two models also show no total increase or decrease in parts of the eastern half of the PRB. CCSM4, on the other hand, shows a total average increase of approximately 120 mm over the basin area.

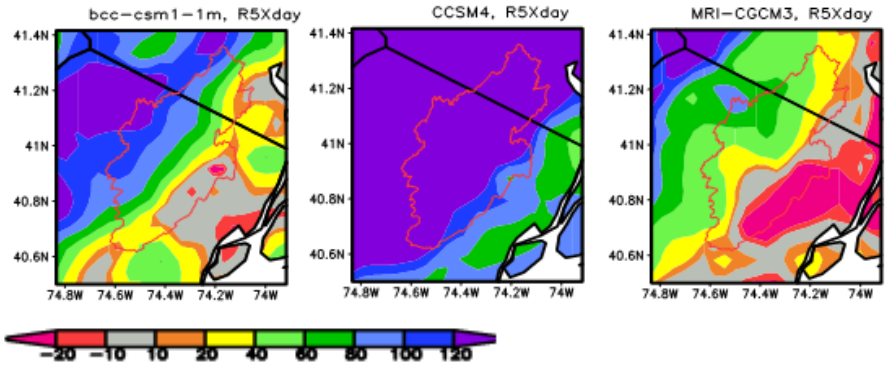

Figure 7 – Projected trends of maximum consecutive 5-day precipitation (mm) for emissions scenario RCP 8.5.

While looking at the results for the climatic extremes, we expected precipitation and temperature extreme indices calculated amongst the models to universally agree that climate indices in RCP 4.5 would show less departure from historic mean results while RCP 8.5 would show more dramatic differences. However, our initial hypotheses were not aligned with model projections. For the 10th percentile of minimum temperature, the models agree that there will less extremely cold days, but RCP 8.5 for bcc-csm1-1m and MRI-CGCM3 shows less of a decrease than RCP 4.5. The models generally also see an increase in the days per year that will experience warmer nights, except in the case of CCSM4 RCP 8.5, which sees a decrease in the 90th percentile of warm nights. Given that there is an overall increase in wet days, extreme precipitation, and consecutive precipitation, we hypothesize that this impact on temperature is due to increased precipitation and associated cloudiness. The increase of rainfall seen by decreased consecutive dry days and the other extreme precipitation indices is most likely due to decreased longwave cooling at nights—therefore, there would be a reduced amount of very cool nights and an increase in warm nights. Elevation may additionally play a role in the east-west differential in expected differences in the climate indices; the PRB houses much of the Highlands in the western half of the basin, and the range of elevation would certainly influence differences in precipitation and temperature.

This study heavily emphasizes the importance of using downscaled GCM climate data to determine the potential impacts of climate change on localities. Figures 5 and 7 both emphasize the potential differences in climate extremes for the PRB. Visualizing the differences in wet days and the differences in heavy precipitation amounts is helpful in delivering detailed climate change analysis. The rainy days are heavily varied within the boundary of the PRB; bcc-csm1-1m shows changes ranging from a decrease of 20 days to an increase of 60-70 days, CCSM4 sees an increase 70 days for the whole basin, while MRI-CGCM3 sees an increase of anywhere from 10 to 70 days. The usefulness of using an RCM can be seen again with the range of differences in the consecutive wet days—the differences amongst the areas in the PRB are defined and clear. Bcc-csm1-m and MRI-CGCM3 see that there is a decrease in the amount of rain the further east you go whereas CCSM4 overall just sees an increase of 130 mm. These differences would not be possible to map without downscaling and bias correcting GCM data.

CONCLUSIONS

The purpose of this study is to identify the ways in which climate change would affect the Passaic River basin by using the MACA model. Many RCMs take information from general circulation models and downscale and bias-correct the data through their own algorithms. When we bias-corrected the model data, we had mixed results from quantile mapping and the delta method and found the more linear method of using a correction factor to improve the model data better than the quantile mapping method.

Using the data to analyze future climatology patterns provided interesting results. The changes in extremes were not consistently further deviating from historic means in the extreme emissions scenarios as compared to the weaker radiative forcing changes. The increase in both precipitation days over 10 mm and the annual precipitation days in which the precipitation exceeded the 95th percentile was expected given the expectations for New Jersey as a whole to experience higher amounts of precipitation. While the results from the models analyzed vary considerably, this study underscores the usefulness of employing downscaled and bias corrected climate projections for investigating plausible future changes at the basin scale.

Future work can extend in different directions. Firstly, incorporating more of the 20 available downscaled, bias corrected MACA models would help create a fuller, more comprehensive understanding of the potential impacts of climate change on the PRB. A sustainability assessment could also be done with the data to help ensure that as the PRB experiences changes, the population experiences socially equitable, economically sustainable, and environmentally sound decision making to increase community resilience. Urban planners and engineers could also use the available projections to incorporate green infrastructure to their plans, creating a more sustainable PRB. We also intend to further this study by assessing impacts of climate change using newer generation CMIP6 models. Ultimately, downscaled, bias corrected GCM data can prove to be very helpful to increase resiliency against climate change for smaller regions.

REFERENCES

Abatzouglou, J. 2013. MACA Methods - Steps. Retrieved from https://climate.northwestknowledge.net/MACA/MACAmethod.php

Chen, J., F. P. Brissette, D. Chaumont, and M. Braun. 2013. Finding appropriate bias correction methods in downscaling precipitation for hydrologic impact studies over North America. *Water Resources Research*. 49(7): 4187-4205.

Christensen, J. H., F. Boberg., O. B. Christensen, and P. Lucas-Picher. 2008. On the need for bias correction of regional climate change projections of temperature and precipitation. *Geophysical Research Letters.* 35(20) L20709, doi:10.1029/2008GL035694.

Dai, A. 2006. Precipitation characteristics in eighteen coupled climate models. *Journal of Climate.* 19(18): 4605-4630.

Eum, H. I., A. J. Cannon, and T. Q. Murdock. 2017. Intercomparison of multiple statistical downscaling methods:multi-criteria model selection for South Korea. *Stochastic Environmental Res Risk Assessment.* 31: 683-703.

Florida, R. 2019. *The Real Powerhouses That Drive the World's Economy*. Bloomberg. https://www.bloomberg.com/news/articles/2019-02-28/mapping-the-mega-regions-powering-the-world-s-economy

Germain, S. J., and J. A. Lutz. 2020. Climate extremes may be more important than climate means when predicting species range shifts. *Climatic Change.* 163(1): 579-598.

Hempel, S., K. Frieler, L. Warszawski, J. Schewe, and F. Piontek. 2013. A trend-preserving bias correction – the ISI-MIP approach. *Earth System Dynamics.* 4: 219-236.

IPCC. 2007. *Climate Change 2007: The Physical Science Basis*. Contribution of Working Group I to the Fourth Assessment Report of the Intergovernmental Panel on Climate Change.

IPCC. 2013. *Climate Change 2013: The Physical Science Basis.* Cambridge: Cambridge University Press.

Karl, T. R., J. M. Melillo, and T. C. Peterson. 2009. *Global Climate Change Impacts in the United States.* Cambridge University Press.

Khajehei, S., A. Ahmadalipour, W. Shao, and H. Moradkhani. 2020. A place-based Assessment of flash flood Hazard and Vulnerability in the contiguous United States. *Scientific Reports*. 10(1): 1-12.

Lafon, T., S. Dadson, G. Buys, and C. Prudhomme. 2013. Bias correction of daily precipitation simulated by a regional climate model: a comparison of methods. *International Journal of Climatology*. 33(6): 1367-1381.

Leander, R., and T. A. Buishand. 2007. Resampling of regional climate model output for the simulation of extreme river flows. *Journal of Hydrology*. 332(3-4): 487-496.

Li, H., J. Sheffield, and E. F. Wood. 2010. Bias correction of monthly precipitation and temperature fields from Intergovernmental Panel on Climate Change AR4 models using equidistant quantile matching. *Journal of Geophysical Research: Atmospheres*. 115(D10).

Marengo, J. A., R. Jones, L. M. Alves, and M. C. Valverde. 2009. Future change of temperature and precipitation extremes in South America as derived from the PRECIS regional climate modeling system. *International Journal of Climatology*. 29: 2241–2255.

Mendez, M., B. Maathuis, D. Hein-Griggs, and L. F. Alvarado-Gamboa. 2020. Performance evaluation of bias correction methods for climate change monthly precipitation projections over Costa Rica. *Water.* 12(2): 482.

Murphy, J. M., D. M. Sexton, D. N. Barnett, G. S. Jones, M. J. Webb, M. Collins, and D. A. Stainforth. 2004. Quantification of modelling uncertainties in a large ensemble of climate change simulations. *Nature*. 430(7001): 768-772.

NASA. 2021. 2020 Tied for Warmest Year on Record, NASA Analysis Shows. Release 21-005. https://www.nasa.gov/press-release/2020-tied-for-warmest-year-on-record-nasa-analysis-shows. Accessed 21 January 2021.

Ngai, S. T., F. Tangang, and L. Juneng. 2017. Bias correction of global and regional simulated daily precipitation and surface mean temperature over Southeast Asia using quantile mapping method. *Global and Planetary Change.* 149: 79-90.

Peterson, T. C., R. R. Heim, and R. Hirsch. 2013. Monitoring and understanding changes in heat waves, cold waves, floods, and droughts in the United States: State of knowledge. *Bull Amer Meteorol Soc.* doi:10.1175/BAMS-D-12-00066.1.

Piani, C., J. O. Haerter, and E. Coppola. 2010. Statistical bias correction for daily precipitation in regional climate models over Europe. *Theor Appl Climatol.* 99:187–192. https://doi.org/10.1007/s00704-009-0134-9.

Räty, O., J. Räisänen, and J. S. Ylhäisi. 2014. Evaluation of delta change and bias correction methods for future daily precipitation: intermodel cross-validation using ENSEMBLES simulations. *Climate Dynamics.* 42(9-10), 2287-2303.

Sharma, D., A. das Gupta, and M. S. Babel. 2007. Spatial disaggregation of bias-corrected GCM precipitation for improved hydrologic simulation: Ping River Basin, Thailand. *Hydrology and Earth System Sciences Discussions*. 11(4):.1373-1390.

Thibeault, J. M., and A. Seth. 2014. Changing climate extremes in the Northeast United States: observations and projections from CMIP5. *Climatic Change*. 127: 273-287.

United States Environmental Protection Agency. 2017. Climate Impacts in the Northeast [Online]. Available: https://19january2017snapshot.epa.gov/climate-impacts/climate-impacts-northeast_.html#:~:text=Between%201958%20and%202012%2C%20the,northern%20parts%20of%20the%20region. [Accessed 22 April 2021].

Vogel, E., M. G. Donat, L. V. Alexander, M. Meinshausen, D. K. Ray, D. Karoly, and K. Frieler. 2019. The effects of climate extremes on global agricultural yields. *Environmental Research Letters.* 14(5): 054010.

Watanabe, S., S. Kanae, S. Seto, P. J. F.Yeh, Y. Hirabayashi,, and T. Oki. 2012. Intercomparison of bias-correction methods for monthly temperature and precipitation simulated by multiple climate models. *Journal of Geophysical Research: Atmospheres.* 117(D23).

Yun, K. S., S. W. Yeh, and K. J. Ha. 2016. Inter-El Niño variability in CMIP5 models: Model deficiencies and future changes. *Journal of Geophysical Research*. 121(8): 3739-4332.

Zhang, X., L. Alexander, G. C. Hegerl, P. Jones, A. K. Tank, T. C. Peterson, and F. W. Zwiers. 2011. Indices for monitoring changes in extremes based on daily temperature and precipitation data. *Climate Change.* 2(6): 851-870.